Cell

Article

Circadian Enhancers Coordinate Multiple Phases of Rhythmic Gene Transcription In Vivo

Bin Fang,[1,2] Logan J. Everett,[1,2] Jennifer Jager,[1,2] Erika Briggs,[1] Sean M. Armour,[1] Dan Feng,[1] Ankur Roy,[1] Zachary Gerhart-Hines,[1] Zheng Sun,[1] and Mitchell A. Lazar[1,*]

[1]Division of Endocrinology, Diabetes, and Metabolism, Department of Medicine, Department of Genetics, and The Institute for Diabetes, Obesity, and Metabolism, Perelman School of Medicine, University of Pennsylvania, Philadelphia, PA 19104, USA

[2]Co-first author

*Correspondence: lazar@mail.med.upenn.edu

http://dx.doi.org/10.1016/j.cell.2014.10.022

SUMMARY

Mammalian transcriptomes display complex circadian rhythms with multiple phases of gene expression that cannot be accounted for by current models of the molecular clock. We have determined the underlying mechanisms by measuring nascent RNA transcription around the clock in mouse liver. Unbiased examination of enhancer RNAs (eRNAs) that cluster in specific circadian phases identified functional enhancers driven by distinct transcription factors (TFs). We further identify on a global scale the components of the TF cistromes that function to orchestrate circadian gene expression. Integrated genomic analyses also revealed mechanisms by which a single circadian factor controls opposing transcriptional phases. These findings shed light on the diversity and specificity of TF function in the generation of multiple phases of circadian gene transcription in a mammalian organ.

INTRODUCTION

A substantial proportion of mammalian genes are expressed with a circadian rhythm driven by a cell autonomous molecular clock (Hughes et al., 2009; Miller et al., 2007; Panda et al., 2002). The clock mechanism involves a network of transcriptional-translational feedback loops comprised of core transcriptional activators BMAL1/CLOCK and two sets of repressors, PER/CRY (Reppert and Weaver, 2001; Takahashi et al., 2008) and Rev-erbs α and β (Bugge et al., 2012; Cho et al., 2012; Ripperger and Schibler, 2001). Under normal conditions, each cellular clock is synchronized by systemic cues and generates multiple phases of rhythmic output (Asher and Schibler, 2011; Dibner et al., 2010; Peek et al., 2012).

Although each circadian transcription factor (TF) binds DNA with genome-wide oscillation peaking at a specific time (Feng et al., 2011; Koike et al., 2012; Rey et al., 2011), binding of an individual circadian TF, e.g., BMAL1, has been reported at genes oscillating with a range of phases, many of which do not correlate with the circadian regulator's binding phase (Menet et al., 2012). Moreover, genome-wide studies have revealed a substantial portion of circadian TF binding tens to hundreds of kilobases away from known transcription start sites (TSS) (Feng et al., 2011; Koike et al., 2012; Rey et al., 2011) and a high degree of overlap between core clock TFs with competing effects on circadian rhythms, such as BMAL1 and Rev-erbα (Cho et al., 2012; Koike et al., 2012). Furthermore, several clock output TFs have been suggested to generate transcriptional rhythms with delayed phase relative to BMAL1/CLOCK, but these mechanisms have not been explored genome-wide (Asher and Schibler, 2011). Thus, a fundamental question remains as to how the interaction of multiple regulators at the genome, particularly at distal enhancer elements, produces distinct phases of circadian transcriptional activity.

Here, we applied Global Run-On sequencing (GRO-seq) (Core et al., 2008; Wang et al., 2011) to mouse livers collected at multiple times of day to measure the circadian activity of enhancer regions based on enhancer RNA (eRNA) transcription (Hah et al., 2013; Kim et al., 2010). We identified thousands of oscillating enhancers with varying peak activity times, and in particular, we found that specific phases of oscillation are associated with distinct regulatory motifs and TF binding patterns. Our data suggest that specific phases of enhancer activity in vivo are achieved by a dominant regulator at each site, determined in part by sequence content, in contrast to combinatorial regulation models based primarily on synthetic in vitro models (Ukai-Tadenuma et al., 2008). Furthermore, we show that eRNA oscillations are highly predictive of the rhythmicity and phase of transcription at nearby genes, demonstrating a large-scale and previously unexplored role for distal regulatory elements in the generation of transcriptional rhythms. By combining circadian enhancer maps, transcription factor cistromes, and genetic ablation of *Rev-erbα* and *Clock*, we demonstrate that circadian eRNAs can be used to both identify the TFs coordinating specific phases of gene transcription and, importantly, uniquely distinguish the functional binding sites within a circadian TF cistrome. Thus, an integrative approach using multiple genomic techniques provides the most detailed and robust model to explain the generation and coordination of multiple phases of rhythm within a single tissue.

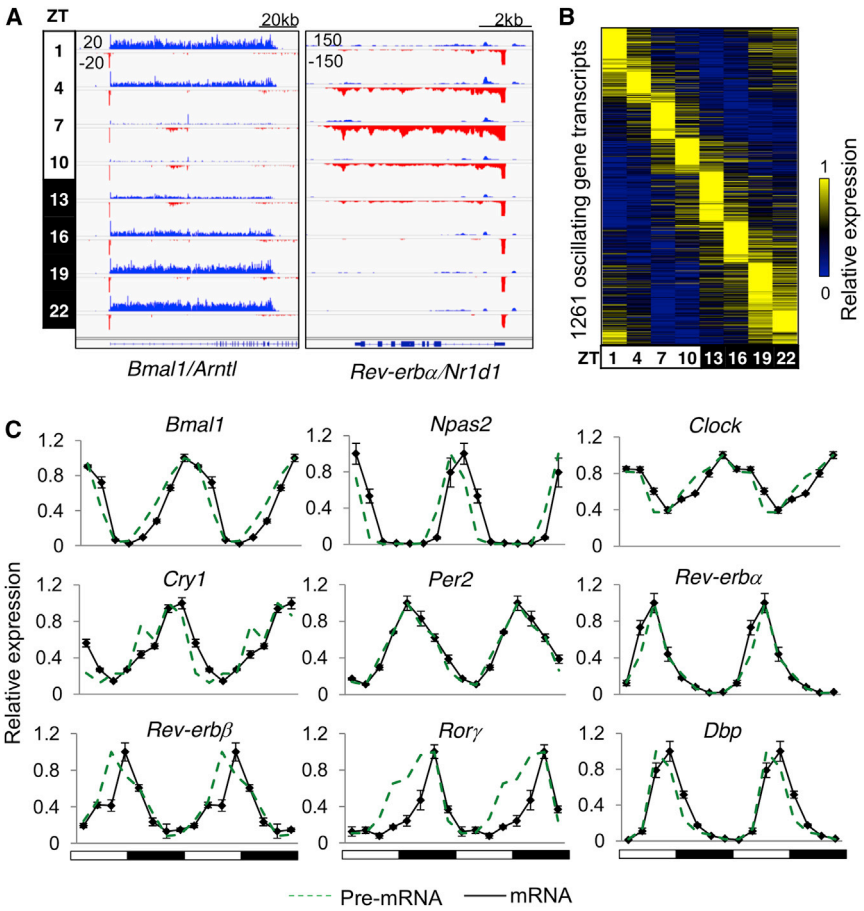

Figure 1. Circadian Transcription in Mouse Liver

(A) Genome browser view of nascent transcripts at *Bmal1/Arntl* and *Rev-erbα/Nr1d1* loci at eight time points. GRO-seq signals on the + and − strand are illustrated in blue and red, respectively. Y axis scale refers to the normalized tag count per million reads.

(B) Heat map of the relative transcription of 1,261 oscillating genes sorted by oscillation phase.

(C) Relative expression of pre-mRNA (green) and mRNA (black) determined by GRO-seq and RT-qPCR, respectively, throughout the day. Data are double plotted for better visualization. RT-qPCR data are expressed as the mean ± SEM (n = 3–4 per time point) and normalized to the maximal expression of the day.

See also Figure S1 and Table S1.

RESULTS

Circadian Transcription in Mouse Liver

GRO-seq was performed on mouse liver nuclei collected every three hours throughout a 24 hr light-dark cycle. Transcription of known circadian genes showed robust oscillation patterns, exemplified by *Bmal1* (*Arntl*) and *Rev-erbα* (*Nr1d1*) (Figure 1A). A total of 11,288 active gene transcripts were identified, of which 1,261 (11%) were transcribed with oscillating patterns (JTK_CYCLE [Hughes et al., 2010], $p < 0.01$, $21 \leq$ period (τ) ≤ 24 hr, peak to trough ratio > 1.5) (Figure 1B; Table S1A available online). Rhythmic mRNA expression of known circadian genes determined by RT-quantitative PCR (RT-qPCR) was associated with their nascent transcription (Figure 1C), and biological replicates of GRO-seq samples at Zeitgeber Time (ZT) 10 and ZT22 showed a high degree of correlation (Pearson correlation coefficient, $r = 0.95$) (Figure S1A). In addition, genes oscillating in similar phases showed closely related biological functions (Figure S1B; Table S1B). Together, these results demonstrate the robustness of our data.

De Novo Identification of Circadian Liver Enhancer RNAs

Analysis of the liver GRO-seq data revealed eRNA transcription in both inter- and intragenic regions, exemplified by highlighted regions in the vicinity of *Pparα* and *Cry2*, respectively (Figure 2A). To globally identify eRNA loci, we developed a pipeline to search for genomic locations producing bi- and unidirectional short RNA transcripts (Extended Experimental Procedures), which identified 19,086 high confidence de novo eRNA loci (>300 bp from TSS) (Table S2A). The average GRO-seq signal of de novo eRNAs showed a bimodal profile in both inter- and intragenic regions (Figure 2B). Analysis of public chromatin immunoprecipitation sequencing (ChIP-seq) data (Table S2B) from mouse liver suggested that de novo eRNA loci were enriched for other epigenomic features including H3K27ac, H3K4me1, DNase I hypersensitivity, and RNA polymerase II (Pol2) recruitment, consistent with the function of these sites as enhancers (Figure 2C). eRNA signals correlated with Pol2 occupancy and histone acetylation but not histone methylation (Figure S2A), consistent with earlier reports (Hah et al., 2013; Li et al., 2013; Wang et al., 2011) and in agreement with the notion that H3K4me1 and H3K27ac mark enhancer identity and activity, respectively (Creyghton et al., 2010).

To examine dynamics of eRNA transcription across the 24 hr cycle, eRNA transcripts were quantified using GRO-seq tag counts within ±500 bp from the centers of eRNA loci. Remarkably, 5,724 (30%) of eRNAs were found to be transcribed in a circadian manner (JTK_CYCLE, $p < 0.05$, $21 \leq$ period (τ) ≤ 24 hr, peak to trough ratio > 1.5) (Table S2C), and their relative expression peaked at different times of the day (Figure 2D). Based on their peak expression time (hereafter referred to as "phase"), circadian eRNAs were divided into eight groups (phase ZT0–ZT24, at 3 hr intervals), represented by eight colors in Figure 2D. Interestingly, circadian eRNAs were not evenly distributed across the eight phase groups. A total of 71% of circadian eRNAs oscillated with a phase between ZT18 and ZT3, whereas 29% of circadian eRNAs oscillated in other phases (Figure 2E; Table S2C). Examples of circadian eRNAs with phase

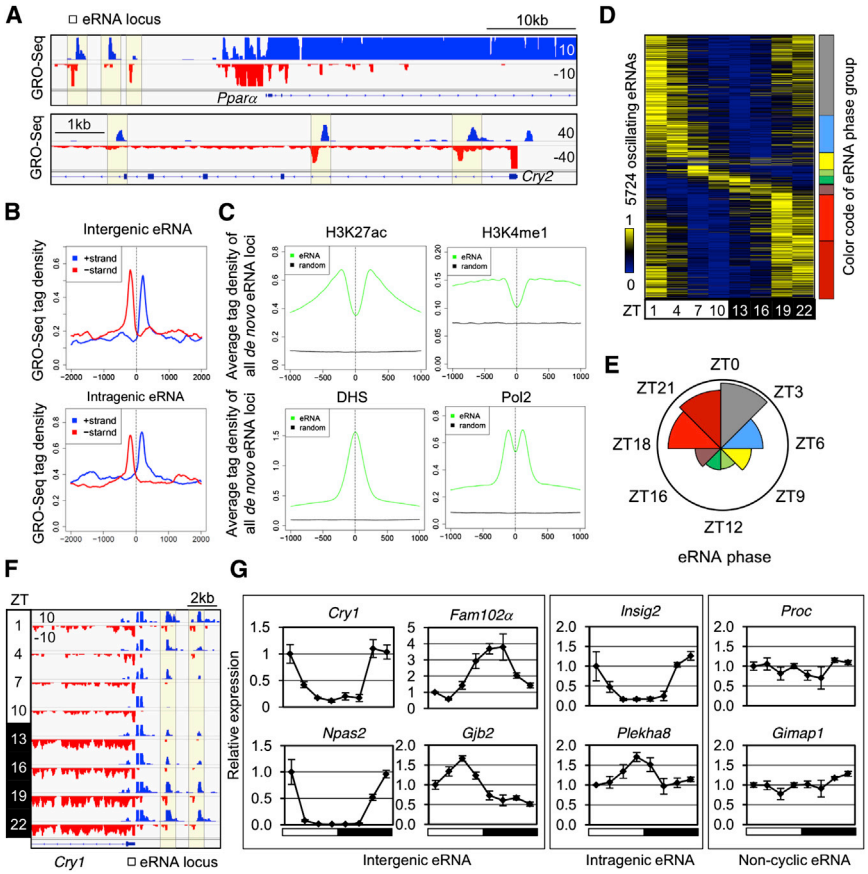

Figure 2. De Novo Identification of Circadian Liver Enhancer RNAs

(A) Genome browser view of intergenic (upper panel) and intragenic (lower panel) eRNAs (yellow boxes).

(B) GRO-seq tag densities in 4 kb windows surrounding de novo intergenic (upper panel) and intragenic (lower panel) eRNA loci are shown for the plus (blue) and minus (red) strand. Y axis shows average reads per 10 million reads (RPTM) per 10 bp bin.

(C) Average ChIP-seq tag densities of epigenetic marks in 2 kb window surrounding all de novo eRNA loci (prior to the selection of high confidence eRNAs) and matched control regions.

(D) Heat map of the relative transcription of oscillating eRNAs throughout the day. Color coding of eRNA population in eight phase groups (from ZT0 to ZT24, at 3 hr intervals) is shown on the right.

(E) Rose diagram showing the prevalence of eRNA loci in each phase group. For each wedge, the color corresponds to that in (D) and the area is proportional to the number of eRNAs in that group.

(F) Genome browser view of oscillating eRNAs at *Cry1* locus.

(G) RT-qPCR validation of circadian transcription for intergenic, intragenic, and noncyclic eRNAs at indicated gene loci. Data are expressed as mean ± SEM (n = 3–4 per time point) and normalized to the first time point.

See also Figure S2 and Table S2.

ZT22 at the *Cry1* locus are shown in Figure 2F. eRNA transcripts oscillating in different phases were confirmed by RT-qPCR (Figure 2G) at selected intergenic and intragenic eRNA loci (Figure S2B). The unbalanced phase distribution of eRNAs agrees with the previous finding that histone acetylation, a reflection of enhancer activity, was globally high around ZT22 and low around ZT10 in the mouse liver (Feng et al., 2011). Moreover, the average H3K27ac level at eight groups of eRNA loci showed the same oscillatory pattern as the circadian eRNAs within each group (Figure S2C). Therefore, circadian eRNAs oscillate in diverse phases, suggesting that circadian enhancer activities are orchestrated by distinct mechanisms in liver.

Phase-Specific Transcription Factors at Circadian Enhancers

We have shown that gene body and eRNA transcription occur in multiple phases. As previous studies suggested correlated transcription of eRNA and nearby target genes (Core et al., 2008; Hah et al., 2013; Kim et al., 2010), we examined whether eRNA oscillations are related to circadian gene transcription. The expression of genes mapped closest to oscillating eRNAs (within 200 kb from TSS) showed rhythmic patterns in phase with eRNA expression (Figure 3A). Among all genes mapped to circadian eRNAs, 423 (34%) circadian gene transcripts were mapped to 1,124 (20%) circadian enhancers and oscillation phases between each enhancer-gene pair were highly correlated (r = 0.9) (Figure S3A). This is likely an underestimate based on the stringent eRNA-gene mapping criteria and, indeed, if the analysis is not limited to the nearest gene, up to 76% of circadian genes in different phases have in-phase eRNAs (phase difference <3 hr between gene and eRNA) located within 200 kb of their TSSs. By contrast, for random genes this number is ~10% on average (hypergeometric test, $p < 0.001$) (Figure S3B). Together, these results suggest that circadian eRNAs predict rhythmic transcription of nearby genes and are likely to be functionally associated with circadian genes of the same phase.

Although gene body and eRNA transcription occur in multiple phases, the core clock oscillator in liver has only one peak and one trough in a 24 hr period (Koike et al., 2012). We considered the possibility that specific circadian TFs were responsible for the different phases of gene expression by driving the transcription of diversely phased eRNAs. To this end, we performed motif analysis on the eight groups of circadian enhancers using 500 bp windows centered on each eRNA locus (Figure S3C). First, candidate phase-specific TFs with the most enriched motifs in each enhancer group were selected by de novo motif mining (Table S3). Then, annotated motifs of candidate TFs were used to quantify the motif enrichment in each enhancer group, revealing four major types of motifs specifically enriched in six enhancer groups (Figure 3B). Specifically, an E-box motif was the most enriched at circadian eRNA loci in phase ZT6–ZT9, coincident with the peak of BMAL1 binding to the genome

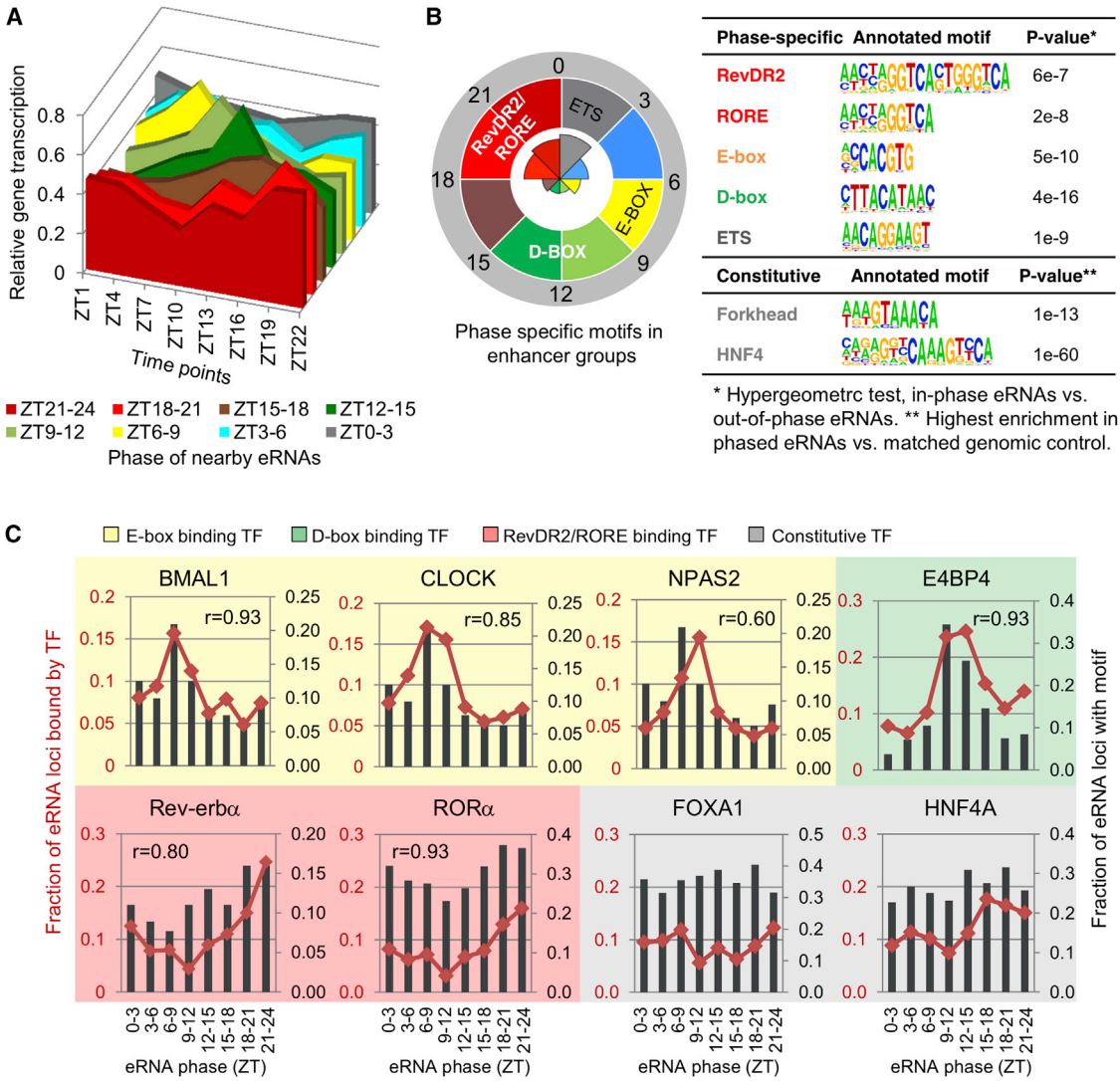

Figure 3. Phase-Specific Transcription Factors at Circadian Enhancers

(A) Relative transcription of genes closest to oscillating eRNAs (within 200 kb of TSS).

(B) Motifs specifically enriched in each eRNA group are labeled in the clock diagram on the left. Position weight matrix (PWM) of each motif and its best enrichment p value in assigned groups are shown in the table on the right.

(C) Correlation of motif occurrence and TF binding in eight eRNA phase groups. In each plot, the red dots represent the fraction of eRNA loci bound by the indicated TF (top 3,000 ChIP-seq peaks), and black bars represent the fraction of eRNA loci containing the corresponding motif. Correlation coefficient r is shown for phase-specific motifs. TFs recognizing different types of motifs are grouped in colored boxes corresponding to those used for eRNA phases.

See also Figure S3 and Table S3.

(Koike et al., 2012; Rey et al., 2011; Ripperger and Schibler, 2006). However, although BMAL1/CLOCK has been previously linked to circadian gene regulation in liver, the ZT6–ZT9 eRNAs comprised only ~6% of circadian enhancers, consistent with an earlier study in which only ~5% of total circadian genes were transcribed in phase with nearby BMAL1 binding (Menet et al., 2012).

We also discovered that a D-box motif, recognized by PAR-bZIP proteins including DBP, TEF, HLF, and E4BP4 (Cowell et al., 1992; Li and Hunger, 2001; Mitsui et al., 2001), was the most enriched motif at phase ZT9–ZT15 eRNA loci (Figure 3B), coinciding with the phase of known target genes for these TFs (Gachon et al., 2006). Moreover, the RevDR2 and RORE motifs, bound by Rev-erbα/β (Harding and Lazar, 1995) and RORα/γ (Giguère et al., 1994), were the top motifs at eRNA loci with the most common phase, ZT18–ZT24 (Figure 3B), coinciding with the trough of repression by Rev-erbα (Bugge et al., 2012; Feng et al., 2011). By contrast, motifs characteristic of ETS binding sites were highly enriched in the phase ZT0–ZT3 enhancers, implying a potential role of ETS proteins in the circadian regulation of transcripts with this phase (Figure 3B). In addition to these phase-specific motifs, constitutively enriched motifs in all

enhancer groups were identified, most prominently the Forkhead and HNF4 motifs (Figure 3B).

We tested whether the motif enrichment in a given eRNA group was predictive of TF binding by overlapping each group of circadian eRNAs with TF cistromes determined by ChIP-seq. Specifically, we analyzed previously published cistrome data for core clock TFs (Feng et al., 2011; Koike et al., 2012) and performed additional ChIP-seq experiments for E4BP4 and RORα. To minimize the effects of variable ChIP-seq quality in different studies, only the 3,000 strongest ChIP-seq peaks for each TF were used in the analysis. Notably, the genomic binding sites of E-box-binding factors BMAL1, CLOCK, and NPAS2 were enriched at eRNAs with phase ZT6–ZT9 (Figure 3C), where de novo analysis implicated the E-box motif. Similarly, genomic binding of Rev-erbα and RORα was enriched at eRNAs whose transcription peaked at ZT21–ZT24 (Figure 3C), where the RevDR2 and RORE motifs were most prominent. Also consistent with the bioinformatic predictions, the D-box binding factor E4BP4 bound most commonly at eRNAs with phase ZT9–ZT15 (Figure 3C). By contrast, binding of FOXA1 and HNF4A, whose motifs were equally enriched in all eRNA groups, did not display a preference for eRNA loci of a specific phase (Figure 3C). Thus, the regulatory activities of six TFs coincide with the rhythmic eRNA expression in the enhancer group at which they were enriched. These data strongly suggest that TFs bound specifically at each enhancer group are potential drivers of their circadian transcription and enhancer activities.

Phase Correlation between eRNA and Gene Body Transcription Marks Functional Enhancers of Circadian Genes

We next considered whether the specific TFs found to bind at circadian enhancers were driving transcription of nearby in-phase genes, focusing on the most common circadian enhancers (phase ZT18–ZT24). Within 200 kb of 325 circadian genes in phase ZT18–ZT24, 539 neighboring eRNA loci showed circadian eRNA transcription in phase ZT18–ZT24 ("correlated enhancers"), while 857 eRNA loci did not produce correlated eRNA transcription ("noncorrelated enhancers," eRNA expression ZT22/ZT10 < 1.5) (Figure 4A).

Correlated enhancers showed higher enrichment of the RevDR2 and RORE motifs in comparison to noncorrelated enhancers (Figure 4B). Notably, relative enrichment of the RevDR2 motif, which is a preferential binding site for Rev-erbα (Harding and Lazar, 1995; Zhao et al., 1998) was 2-fold higher than that of the RORE motif shared by Rev-erbα and RORα (Giguère et al., 1994), suggesting that Rev-erbα may play a more important role in regulating the correlated enhancers. ChIP-seq tag densities of Rev-erbα and its corepressor HDAC3 were dramatically stronger at correlated enhancers than at noncorrelated enhancers (Figure 4C), supporting the idea that the correlated enhancers in phase ZT18–ZT24 were controlled by Rev-erbα. To test this hypothesis, GRO-seq was performed on livers from mice genetically lacking Rev-erbα (*Rev-erbα*$^{-/-}$) at ZT10, when Rev-erbα levels normally peak and maximally repress histone acetylation and gene transcription (Feng et al., 2011). Indeed, eRNA signals at the correlated enhancers were markedly derepressed in *Rev-erbα*$^{-/-}$ mice, while no such change was seen at the noncorrelated enhancers (Figure 4D). Similar results were obtained at both inter- and intragenic enhancers (Figure S4). Importantly, gene body transcription that normally peaked at ZT18–ZT24 was also extensively derepressed in *Rev-erbα*$^{-/-}$ mice at ZT10 (Figure 4E), indicating these genes are direct targets of Rev-erbα. Together, these results demonstrate that eRNAs in phase ZT18–ZT24 mark functional Rev-erbα binding sites that regulate neighboring target genes with correlated phase. Conversely, noncorrelated enhancers are not bound by Rev-erbα and do not control Rev-erbα target genes.

Circadian eRNAs Reveal the Functional Rev-erbα Cistrome at Oscillating Genes

The findings to this point demonstrate that Rev-erbα regulates circadian genes in phase ZT18–ZT24 via enhancers oscillating in phase with gene body transcription. However, these enhancers account for only a small fraction of the complete Rev-erbα cistrome (Feng et al., 2011). We therefore considered whether circadian eRNAs in phase ZT18–ZT24 uniquely mark the functional subset of Rev-erbα binding sites controlling circadian genes in liver. To test this, Rev-erbα sites near circadian genes were divided into three groups, of which 887 (33%) overlapped de novo eRNA loci, 347 (13%) were found at TSSs of circadian genes (within 300 bp), and the remaining 1,455 (54%) were not associated with detectable eRNA transcription (Figure 5A). Of the eRNAs transcribed at Rev-erbα binding sites, 30% peaked at ZT18–ZT24, while 19% peaked in other phases, and 51% were constitutively expressed eRNA and did not oscillate (Figure 5A).

Rev-erbα and its corepressor HDAC3 bound more strongly at sites producing ZT18–ZT24 eRNAs than at other types of binding sites (Figure 5B), resulting in a marked decrease in histone H3K9 acetylation from ZT22 to ZT10 (Figure S5). To directly assess the functionality of Rev-erbα binding on individual gene expression, we constructed a list of high confidence target genes whose nascent and mature transcripts were derepressed in *Rev-erbα*$^{-/-}$ livers at ZT10 compared to wild-type (WT) (Tables S4A–S4C). The enrichment of derepressed circadian genes in *Rev-erbα*$^{-/-}$ mice was >3-fold higher near Rev-erbα sites producing ZT18–ZT24 eRNAs, compared to other Rev-erbα sites (Figure 5C), suggesting that ZT18–ZT24 eRNAs mark functional Rev-erbα sites. Moreover, circadian genes with phase around ZT21–ZT24 were highly enriched for derepression in *Rev-erbα*$^{-/-}$ mice (Figure 5D), consistent with the enrichment of circadian eRNAs in this phase. Together, these data strongly suggest that only a subset of the Rev-erbα cistrome associated with antiphase eRNAs is functional in controlling circadian gene transcription.

eRNA Analysis Identifies E4BP4 as a Key Mediator of Gene Activation by Rev-erbα

While eRNAs clearly delineate the functional Rev-erbα cistrome responsible for direct transcriptional repression, there remains a substantial set of genes paradoxically downregulated at ZT10 in *Rev-erbα*$^{-/-}$ mouse livers, which cannot be explained through direct regulation by Rev-erbα. To identify factors mediating this opposing effect on gene transcription, we constructed a list of high confidence target genes whose nascent and mature transcript levels were decreased in *Rev-erbα*$^{-/-}$ livers at ZT10

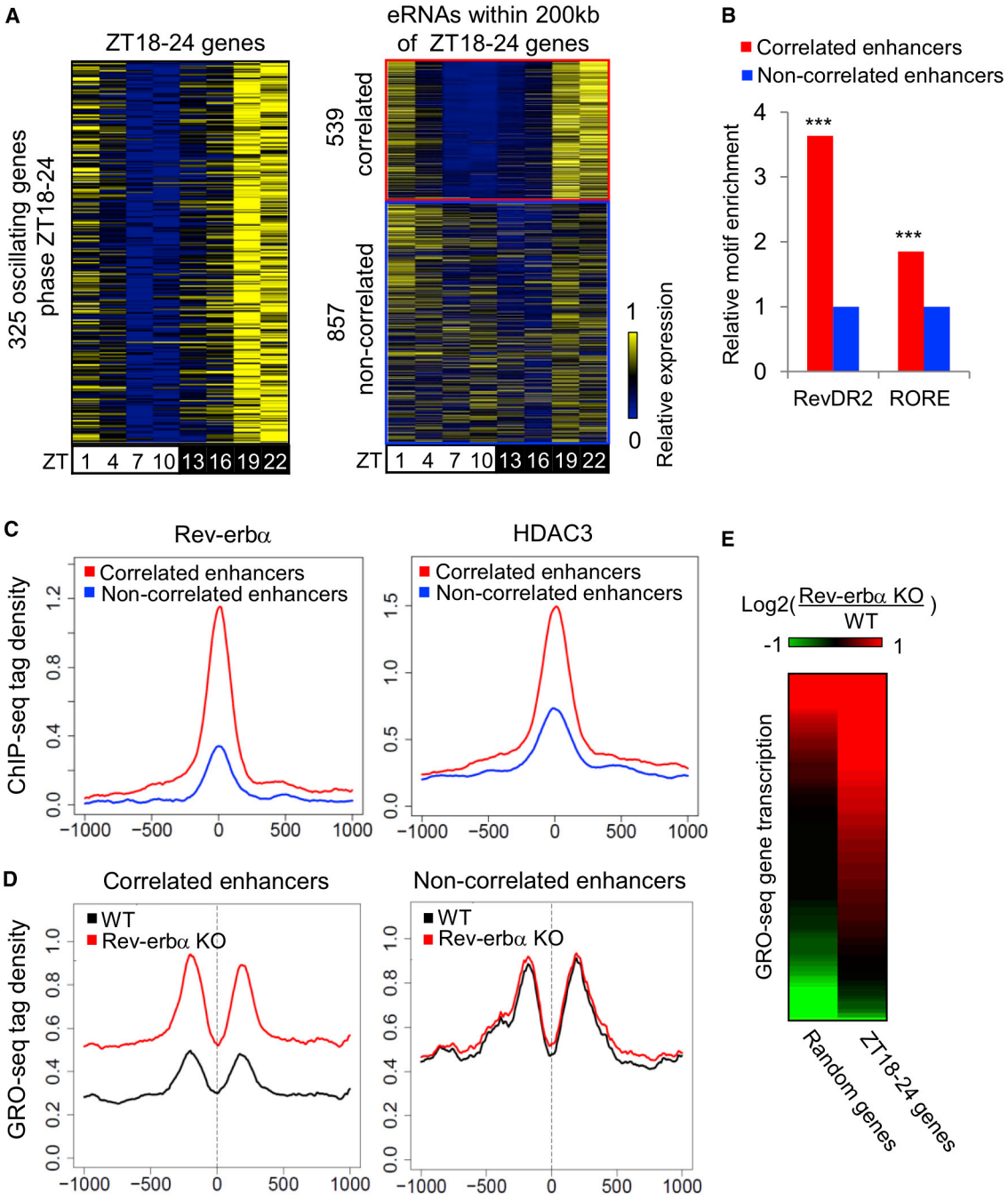

Figure 4. Phase Correlation between eRNA and Gene Body Transcription Marks Functional Enhancers of Circadian Genes

(A) Heatmap of the relative transcription of 325 circadian genes in phase ZT18–ZT24 (left) and their neighboring eRNAs (right). A total of 539 eRNAs in correlated phase are shown in the red box while 857 noncorrelated eRNAs are in the blue box.

(B) Enrichment of RevDR2 and RORE motif in correlated eRNA loci relative to noncorrelated eRNA loci (hypergeometric test, ***$p < 0.001$).

(C) ChIP-seq tag density of Rev-erbα (left) and HDAC3 (right) in 2 kb windows surrounding correlated (red) and noncorrelated eRNA loci (blue). Y axis shows the average tag count per 10 bp bin normalized to 10 million total reads.

(D) Comparison of GRO-seq tag density (RPTM per 10 bp bin in 2 kb window) surrounding correlated (left) and noncorrelated (right) eRNA loci in WT and *Rev-erbα*$^{-/-}$ livers at ZT10.

(E) Heatmap of transcriptional changes between WT and *Rev-erbα*$^{-/-}$ livers at ZT10, for the 325 circadian genes in phase ZT18–ZT24 (right column), compared to the same number of random genes (left column). Data are expressed as log2 fold change.

See also Figure S4.

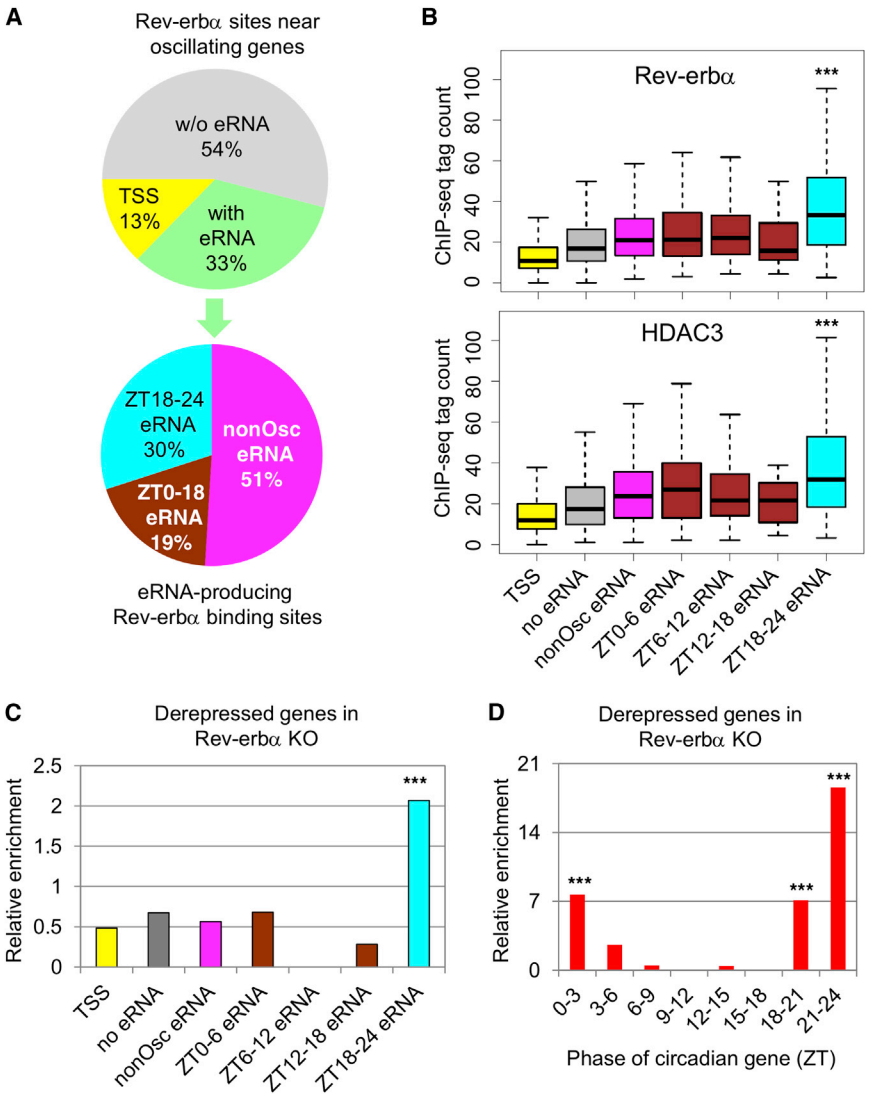

Figure 5. Circadian eRNAs Reveal the Function of the Rev-erbα Cistrome at Oscillating Genes

(A) Distribution of Rev-erbα ChIP-seq peaks near circadian genes (upper panel) and subdistribution of eRNA-producing Rev-erbα peaks near circadian genes (lower panel).

(B) Boxplot showing Rev-erbα and HDAC3 peak height at binding sites from (A). Y axis indicates normalized tag count in each peak (RPTM) (***$p < 0.001$, one-way ANOVA and Tukey's test).

(C) Enrichment of derepressed genes in *Rev-erbα*$^{-/-}$ mice at circadian genes bound by different Rev-erbα peaks from (A) relative to a random set of Rev-erbα peaks (hypergeometric test, ***$p < 0.001$).

(D) Enrichment of derepressed genes in *Rev-erbα*$^{-/-}$ mice in 8 groups of circadian genes with indicated phases relative to randomly selected genes (hypergeometric test, ***$p < 0.001$).

See also Figure S5 and Table S4.

(Tables S4A–S4C). Profiling of eRNAs near genes that were downregulated in the *Rev-erbα*$^{-/-}$ livers revealed a marked and specific enrichment for phases between ZT9 and ZT15 (Figure 6A), which were shown earlier to be enriched for the D-box motif and binding of the D-box repressor E4BP4 (Figure 3C).

We hypothesized that, by controlling the circadian expression of E4BP4, Rev-erbα indirectly dictated the circadian expression of a large set of genes controlled by D-box enhancers whose expression would thus be in phase with Rev-erbα. Indeed, E4BP4 gene expression was circadian in WT mouse livers but constitutively elevated in *Rev-erbα*$^{-/-}$ mice (Figure 6B), consistent with a previous report (Duez et al., 2008). Furthermore, Rev-erbα bound along with its NCoR-HDAC3 corepressor complex to several sites at the *E4BP4* (*Nfil3*) locus, suggesting that E4BP4 expression is directly controlled by Rev-erbα (Figure S6A). By contrast, there were weaker changes in hepatic expression of D-box activating factors *Dbp*, *Tef*, and *Hlf* in livers of *Rev-erbα*$^{-/-}$ mice, and the expression of these factors remained circadian with similar phases (Figure S6B).

To identify putative functional E4BP4 sites, we analyzed the complete set of E4BP4 ChIP-seq peaks for those with higher eRNA levels at ZT9–ZT15 (ZT10/ZT22 > 3 or ZT13/ZT1 > 3). These sites, which we refer to as "E4BP4+eRNA" sites, were enriched 2-fold around genes downregulated in *Rev-erbα*$^{-/-}$ mice (Figure 6C), demonstrating a significant association between E4BP4 binding and gene regulation downstream of Rev-erbα. Transcriptome profiles from livers of WT mice (Hughes et al., 2009) confirmed that putative E4BP4 target genes (downregulated in *Rev-erbα*$^{-/-}$ livers and near E4BP4+eRNA sites) were generally circadian with average peak and trough expression in phase with Rev-erbα and E4BP4 levels, respectively (Figure 6D, green line). The average GRO-seq transcription profile for this same group of genes showed a similar pattern over a 24 hr cycle (Figure 6D, blue line). Both patterns are consistent with direct repression by E4BP4 leading to circadian oscillation in phase with Rev-erbα protein levels. In contrast, Rev-erbα target genes (upregulated in *Rev-erbα*$^{-/-}$ livers and near Rev-erbα sites overlapping ZT18–ZT24 eRNAs) were on average antiphase to Rev-erbα expression in WT livers, consistent with direct transcriptional repression by Rev-erbα (Figure 6E). As a control, genes that were expressed near oscillating eRNAs, but unchanged in the *Rev-erbα*$^{-/-}$ livers, were not systematically phased relative to Rev-erbα or E4BP4 levels (Figure 6F).

These findings support a model in which Rev-erbα indirectly activates genes in phase ZT9–ZT15 by repressing the D-box repressor E4BP4. Such a model predicts that E4BP4 target genes would be constitutively downregulated in *Rev-erbα*$^{-/-}$ livers, with increased E4BP4 binding at nearby functional sites. Indeed, expression profiling over a 24 hr cycle revealed that

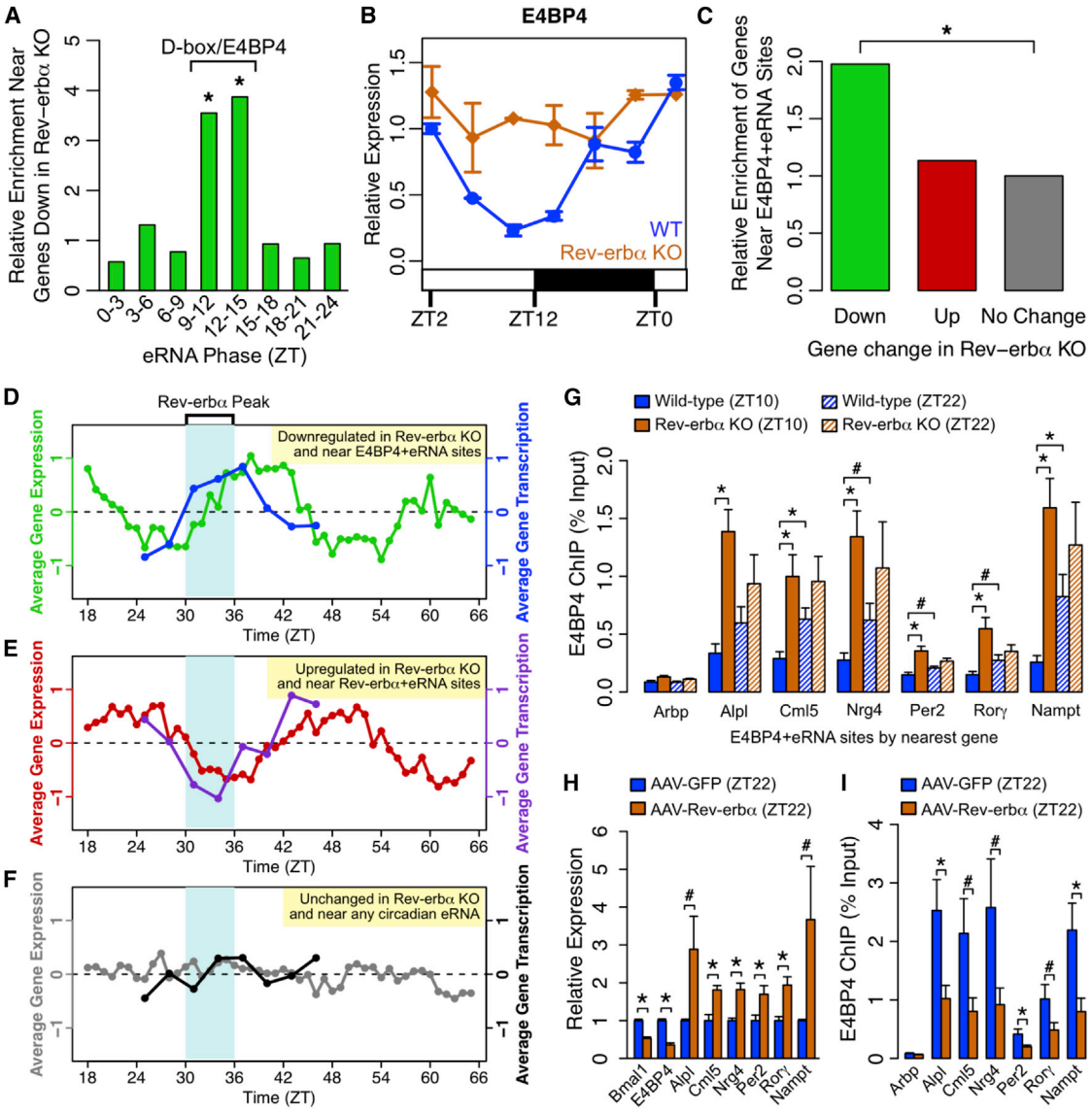

Figure 6. E4BP4 Functions Downstream of Rev-erbα

(A) Enrichment of oscillating eRNAs in each phase group near genes downregulated in *Rev-erbα*$^{-/-}$ livers relative to control genes. Significantly enriched phases are noted as corresponding to D-box/E4BP4-enriched phase group. (hypergeometric test, *p < 0.05).

(B) mRNA expression of *E4BP4/Nfil3* in WT and *Rev-erbα*$^{-/-}$ livers measured by RT-qPCR throughout the day. Data are expressed as mean ± SEM (n = 2 per time point and genotype) normalized to the first WT time point.

(C) Enrichment of E4BP4+eRNA bound genes among those downregulated (green) or upregulated (red) in *Rev-erbα*$^{-/-}$ livers relative to unchanged genes (gray) (hypergeometric test, *p < 0.05).

(D–F) Average circadian expression profiles in WT mouse livers (Hughes et al., 2009) and corresponding transcription profiles by GRO-seq for (D) genes downregulated in *Rev-erbα*$^{-/-}$ livers within 200 kb of E4BP4 binding at ZT9–ZT15 circadian eRNAs, (E) genes upregulated in *Rev-erbα*$^{-/-}$ livers within 200 kb of Rev-erbα binding at ZT18–ZT24 circadian eRNAs, and (F) nonregulated control genes (expressed in liver within 200 kb of circadian eRNA in any phase).

(G) ChIP-qPCR of E4BP4 binding at genes downregulated in *Rev-erbα*$^{-/-}$ livers at ZT10. Binding is shown at ZT10 (solid bars) and ZT22 (hashed bars) in WT (blue) and *Rev-erbα*$^{-/-}$ (orange) livers. Data are expressed as mean ± SEM (one-way ANOVA, *p < 0.05, $^{\#}$p < 0.1, n = 3–4 per group).

(H) mRNA expression measured by RT-qPCR in liver overexpressing Rev-erbα (mice injected with AAV-Tbg-Rev-erbα) or control liver (mice injected with AAV-Tbg-GFP) at ZT22. Data are expressed as mean ± SEM (one-way ANOVA, *p < 0.05, $^{\#}$p < 0.1; n = 6 per group).

(I) ChIP-qPCR of E4BP4 binding at same sites as (G) in liver overexpressing Rev-erbα (orange) or control liver (blue). Data are expressed as mean ± SEM (one-way ANOVA, *p < 0.05, $^{\#}$p < 0.1, n = 5–6 per group).

See also Figure S6.

genes near E4BP4+eRNA sites showed attenuated rhythmic expression in *Rev-erbα*$^{-/-}$ livers (Figure S6C). Furthermore, E4BP4 genomic binding was increased at ZT10 and no longer circadian at these sites in *Rev-erbα*$^{-/-}$ livers (Figure 6G).

We also tested the effect of ectopic expression of Rev-erbα in mouse livers on E4BP4 expression and function. Interrogation of data from a previously published experiment (Kornmann et al., 2007) revealed upregulation of the genes putatively controlled by E4BP4 in livers constitutively expressing Rev-erbα, particularly at the physiological peak time of E4BP4 expression (Figure S6D). Indeed, while constitutive expression of Rev-erbα in mouse liver repressed its direct targets such as *Bmal1* and *E4BP4/Nfil3*, it upregulated E4BP4 target genes at ZT22 (Figure 6H). This effect was much less apparent at ZT10 when E4BP4 is already at physiologically low levels (Figure S6E). Importantly, E4BP4 binding at putative functional sites near these genes was reduced at ZT22, consistent with loss of repression by E4BP4 at the implicated D-box elements (Figure 6I). These results strongly suggest that E4BP4 functions downstream of Rev-erbα, via sites transcribing eRNA in phase ZT9–ZT15, to repress the genes that are downregulated in *Rev-erbα*$^{-/-}$ livers and upregulated when Rev-erbα is overexpressed.

Circadian eRNAs Define Functional Cistromes that Distinguish CLOCK and Rev-erbα Target Genes

CLOCK and Rev-erbα have opposite effects on gene transcription; however, their maximal binding to the genome occur in roughly the same time window (ZT8–ZT10) (Cho et al., 2012; Feng et al., 2011; Koike et al., 2012). ChIP-seq results suggest that 80% of genes bound by CLOCK within 200 kb of TSS were also bound by Rev-erbα (Figure S7A), resulting in 15%–35% of circadian genes in different phases cobound by these two factors (Figure S7B). The question as to how co-occurrence of CLOCK and Rev-erbα binding affects rhythmic gene transcription remains unsolved (Zhao et al., 2014).

Having demonstrated that functional Rev-erbα sites marked by ZT18–ZT24 eRNAs correlated with target gene phase (Figures 4 and 5), we tested whether eRNAs oscillating in other phases could identify the functional cistromes of other clock components. To this end, we analyzed published microarray data measuring gene expression in livers of WT and *Clock* mutant mice (Miller et al., 2007). We first noted that genes downregulated in the *Clock* mutant mice were significantly enriched for circadian eRNAs in the phase ZT6–ZT9 compared to control genes (Figure S7C), corresponding to the enrichment of E-box motif and CLOCK binding. We then selected putatively functional CLOCK sites (Koike et al., 2012) producing eRNAs in phase with CLOCK binding (Table S5, eRNA level ZT7/ZT19 > 3 or ZT10/ZT22 > 3) and correlated with nearby gene transcription and compared these sites to the remainder of the CLOCK cistrome.

Target genes within 200 kb of putatively functional CLOCK sites showed rhythmic mRNA expression in WT mice (Miller et al., 2007), peaking at the time point corresponding to ZT10 in our studies (Figure 7A, yellow line). These genes also showed reduced expression overall in *Clock* mutant mice, particularly at time points corresponding to ZT6 and ZT10 (Figure 7A, orange line). By comparison, genes near other CLOCK sites showed weaker average rhythm and weaker average reduction in *Clock* mutant mice (Figure 7B). Further confirming that CLOCK sites marked by in phase eRNA represent the functional subset of the CLOCK cistrome, target genes near these sites are significantly enriched for circadian genes specifically in phases ZT6–ZT12, but not opposing phases (Figure 7C) and are also significantly enriched for genes downregulated >1.5-fold in *Clock* mutants (Figure 7D). The fact that mRNA levels of some CLOCK target genes cycle in phases ZT9–ZT12 is likely due to delays in the phase of mature mRNA oscillations relative to nascent transcription, as noted in previous studies (Menet et al., 2012). Taken together, these results demonstrate that CLOCK sites marked by in phase eRNAs represent the functional component of the total cistrome.

To examine whether CLOCK and Rev-erbα are both functional at cobound circadian genes, functional binding sites of each factor were mapped to their closest circadian genes. CLOCK binding sites at TSS were included in this analysis as they are also enriched at genes downregulated in *Clock* mutant mouse livers (Figure S7D), consistent with previous studies (Rey et al., 2011). Remarkably, the majority of cobound circadian genes contained functional binding sites of only one factor but not both, with genes around phase ZT6–ZT9 and ZT18–ZT24 most enriched for functional CLOCK and Rev-erbα sites, respectively (Figure 7E). These findings suggest exclusive functions of either CLOCK or Rev-erbα at most cobound genes. Consistent with this notion, expression profiling showed that cobound genes exclusively carrying functional CLOCK sites, such as *Nr1d1*, *Nr1d2*, and *Tef*, are deactivated in *Clock* mutant mice, while those only carrying functional Rev-erbα sites, such as *Cry1* and *E4BP4*, are derepressed in *Rev-erbα*$^{-/-}$ mice (Figures 7F and S7E). Therefore, despite frequent colocalization of their binding, CLOCK and Rev-erbα control distinct sets of circadian genes that can be predicted from their regulation of eRNAs.

DISCUSSION

Unbiased analysis of the nascent transcription of over 5,000 circadian eRNAs and the TF motifs at these sites has allowed us to identify the direct genomic targets of multiple circadian regulators in mouse liver. Circadian eRNA loci are enriched for enhancer marks, the phase of eRNA oscillation correlated with that of nearby genes, and knockout studies demonstrated the causal relationship between TF binding and the transcriptional regulation at enhancers and the genes they control. These results informed the comparison of cistromes with gene expression and thus revealed the functional cistromes of multiple TFs that bind at thousands of genomic sites in liver.

Previous genomic studies of circadian gene regulation have focused primarily on the core clock components BMAL1/CLOCK, which bind DNA with a uniform genome-wide phase peaking at ZT6–ZT9 (Hatanaka et al., 2010; Koike et al., 2012; Menet et al., 2012; Rey et al., 2011; Yoshitane et al., 2014), yet only a small fraction of circadian gene transcription is in this phase. Our data suggest that only the genes with phase ZT6–ZT9 are the true BMAL1/CLOCK targets, while many other genes are bound, but not controlled, by BMAL1/CLOCK possibly due to inactive binding or long distance looping to different genes.

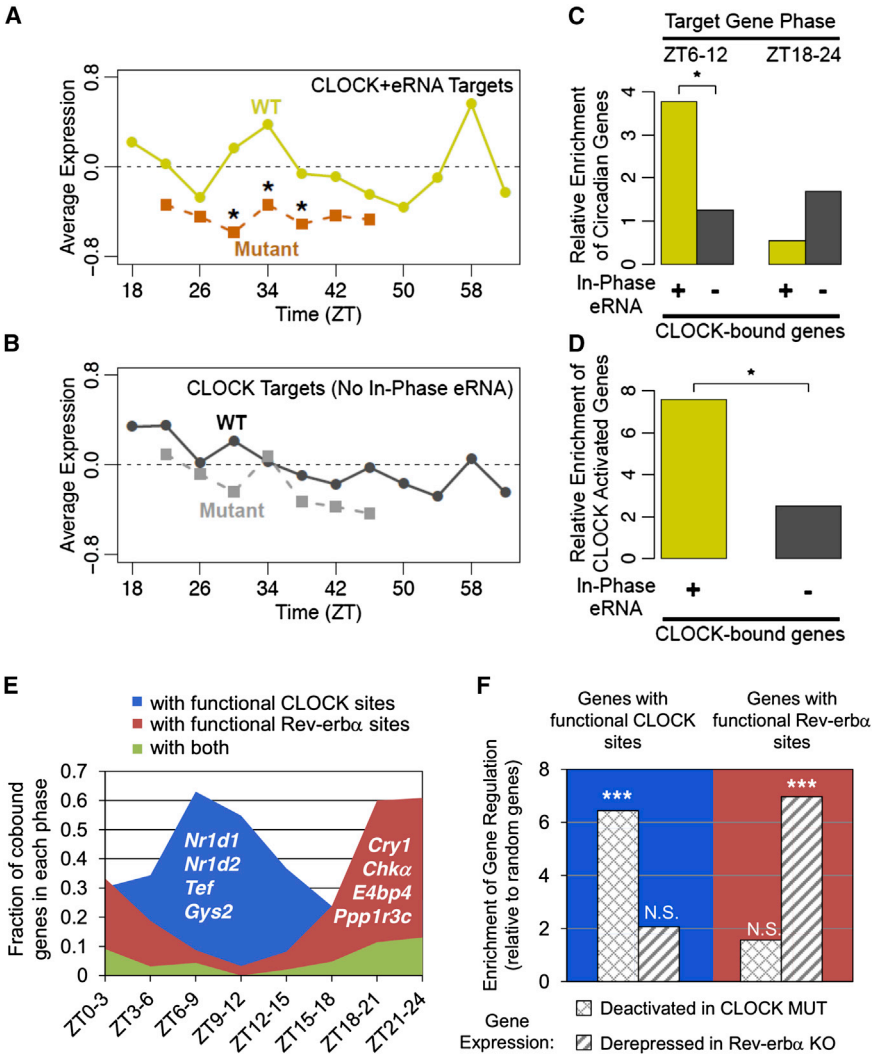

Figure 7. Circadian eRNAs Define Functional Cistromes that Distinguish CLOCK and Rev-erbα Target Genes

(A) Average expression of genes within 200 kb of CLOCK binding sites producing eRNA in phase with CLOCK binding and target gene expression in WT (yellow line) and *Clock* mutant (orange line) mouse livers from Miller et al. (2007) (Wilcoxon test of gene fold-change distribution versus matching time points in (B), *p < 0.05).

(B) Average expression of genes within 200 kb of CLOCK binding sites lacking in-phase eRNA in WT (dark gray line) and *Clock* mutant (light gray line) mouse livers from Miller et al. (2007).

(C) Enrichment of circadian genes expressed in phase with CLOCK binding (ZT6–ZT12) or antiphase to CLOCK binding (ZT18–ZT24) for the gene groups used in (A) (yellow) and (B) (gray) relative to random genes (hypergeometric test, *p < 0.05).

(D) Enrichment of genes downregulated in *Clock* mutant livers among the gene groups used in (A–C) relative to random genes (hypergeometric test, *p < 0.05).

(E) Fraction of oscillating genes cobound by CLOCK and Rev-erbα that are within 200 kb of TF binding sites producing rhythmic eRNA in phase with CLOCK activation (blue), Rev-erbα repression (red), or both (green). Oscillating genes are divided according to their phases. Representative genes are noted in each group.

(F) Enrichment of CLOCK and Rev-erbα regulated genes (expression fold change in mutant >95% of random genes) in those with eRNA predicted functional binding sites in (E), relative to random genes (hypergeometric test, ***p < 0.001, not significant [N.S.] p > 0.05).

See also Figure S7 and Table S5.

Moreover, despite extensive binding region overlap with Rev-erbα (Cho et al., 2012), whose repressive activity would conflict with activation by BMAL1/CLOCK, our results demonstrate on a genome-wide scale that enhancer activity is primarily controlled by one factor or the other.

Importantly, our unbiased identification of enhancers revealed not only the ZT6–ZT9 enhancers marked by E-box motifs and bound by BMAL1, NPAS2, and CLOCK but also more abundant sets of enhancers in other phases. Those peaking at ZT0–ZT3, ZT9–ZT15, and ZT18–ZT24 were enriched for ETS, D-box, and RevDR2/RORE motifs, respectively. The ETS motif is recognized by a large family of TFs (Hollenhorst et al., 2011), some of which have recently been implicated in circadian biology and will be the focus of future research (Anafi et al., 2014; Ciarleglio et al., 2014). Moreover, by integration of enhancer sites with cistromic data, E4BP4 emerged as a key regulator of the ZT9–ZT15 D-box enhancers in normal liver, as well in the *Rev-erbα*$^{-/-}$ livers, and Rev-erbα was clearly a strong antiphase repressor bound to RevDR2/RORE sites at ZT18–ZT24 enhancers.

Interestingly, the phase of circadian enhancers exhibited an uneven distribution, with 42% of circadian eRNAs peaking during the late night (ZT18–ZT24), while rhythmic gene transcription was more evenly distributed across all phases. A possible explanation is that the regulation of genes whose transcription peaks in the light cycle might be primarily regulated at promoters. For example, BMAL1 controls gene transcription at both promoters and enhancers (Rey et al., 2011), whereas Rev-erbα, the main controller of the ZT18-24 phase, binds mainly intergenically (Feng et al., 2011; Lam et al., 2013). The overabundance of enhancers in phase ZT18–ZT24 is surprising, yet remarkably consistent with the previously unexplained finding of Koike et al. (2012) that the global peak of initiated Pol2 occurs at ~ZT22–ZT24.

Analysis of oscillating eRNAs in mice fed normal chow ad libitum did not reveal the motifs for TFs previously suggested to entrain liver circadian gene expression to feeding/fasting cycles, such as CREB, SREBP, PPARs, and FOXO1 (Adamovich et al., 2014; Eckel-Mahan et al., 2013; Vollmers et al., 2009). Some of these TFs, such as CREB and SREBP, bind preferentially to promoters of target genes (Everett et al., 2013; Gilardi et al., 2014; Seo et al., 2009), which would not be captured by analysis of

eRNAs. Phase-specific enrichment could also have been masked by motifs bound by constitutive liver TFs, such as HNF4A and FOXA1, that bind at enhancers in all phases. It will be interesting to profile eRNAs under altered dietary conditions in future studies to examine the interplay between metabolic cues and circadian rhythms at enhancers.

Rev-erbα expression and repressive function peaks at ZT10 in liver, thereby orchestrating circadian transcription in the opposing phase (ZT22) (Feng et al., 2011). Consistent with this, recruitment of Rev-erbα and its corepressor was strongest at sites of ZT18–ZT24 eRNA transcription. It should be noted that the entire Rev-erbα cistrome in liver includes thousands of other binding sites, with <10% characterized by rhythmic eRNAs antiphase to Rev-erbα binding. Deletion of Rev-erbα specifically activated transcription of these eRNAs, as well as the genes they control, thus clearly delineating the functional component of the Rev-erbα cistrome.

In addition to the direct regulation of circadian genes antiphase to Rev-erbα expression, we uncovered a large set of in-phase circadian transcripts that were downregulated in the absence of Rev-erbα, contrary to its powerful repressive function. Functional enhancer analysis suggested that the downregulated genes in *Rev-erbα*$^{-/-}$ mice were mediated by D-box factors, including E4BP4, a direct target of Rev-erbα. While the direct regulation of E4BP4 by Rev-erbα has been recognized (Duez et al., 2008), a relatively small number of E4BP4 target genes have been identified in liver, based primarily on in vitro studies of proximal promoter constructs (Tong et al., 2010; Ueda et al., 2005). Our study includes a ChIP-seq study of E4BP4 in liver, and our integrative analysis demonstrates the extensive, genome-wide effects of this pathway, revealing how a single TF, such as Rev-erbα, can regulate opposing phases of circadian gene expression by its direct and indirect actions.

Together, the present studies reveal mechanisms for generating and coordinating multiple phases of circadian transcription in a single organ. They also demonstrate that the unbiased analysis of enhancer activity and correlated gene expression is a powerful method of discovering relevant TFs and their specific functional cistromes, which can be more generally applied to understanding the transcriptional regulation of physiology and disease states.

EXPERIMENTAL PROCEDURES

Mice

WT C57Bl/6 mice were purchased from the Jackson Laboratories. The *Rev-erbα*$^{-/-}$ mice were obtained from B. Vennström and backcrossed greater than or equal to seven generations with C57Bl/6 mice. WT and mutant male mice (10- to 12-week-old) were housed under standard 12 hr light/12 hr dark cycles, with lights on (ZT0) at 7 a.m. and lights off (ZT12) at 7 p.m. and euthanized at indicated times. All animal care and procedures followed the guidelines of the Institutional Animal Care and Use Committee of the University of Pennsylvania.

Antibodies

E4BP4 antibodies (Santa Cruz sc-9550 and sc-9549) were mixed in 1:1 ratio for ChIP. RORα antibody was purchased from Santa Cruz (sc-6062).

GRO-Seq

The GRO-seq was performed as previously described (Core et al., 2008; Step et al., 2014; Wang et al., 2011). Raw data are available in Gene Expression Omnibus (GEO) (GSE59486). See also Extended Experimental Procedures.

De Novo Identification of eRNAs

A pipeline was constructed for genome-wide de novo identification of eRNA loci. See also Extended Experimental Procedures.

Analysis of Oscillating Gene Transcripts and eRNAs

RPKTM values across all time points for each transcript and eRNA feature were analyzed for significant circadian oscillations using JTK_CYCLE (Hughes et al., 2010). Motif mining at oscillating eRNAs was performed by applying HOMER to the 500bp window centered on each locus. See also Extended Experimental Procedures.

Gene and eRNA Expression Analysis

Total RNA was extracted from liver using the RNeasy Mini Kit (QIAGEN) and treated with DNase (QIAGEN). RNA was reverse transcribed using the High-Capacity cDNA Reverse Transcription Kit (Applied Biosystems). Quantitative PCR was performed with Power SYBR Green PCR Mastermix on the PRISM 7500 (Applied Biosystems) and analyzed by the standard curve method. Gene or eRNA expression was normalized to mRNA levels of housekeeping gene *36B4* (*Arbp*). Primer sequences can be found in Table S1D.

Microarray Analysis

Microarray analysis of WT and *Rev-erbα*$^{-/-}$ livers (n = 5) was performed by the Penn Microarray Core. Raw data are available from GEO (GSE59460). See also Extended Experimental Procedures.

ChIP

ChIP-qPCR and ChIP-seq experiments were performed as described (Feng et al., 2011) with minor changes. Raw data for RORα and E4BP4 ChIP-seq are available in GEO (GSE59486). See also Extended Experimental Procedures.

ChIP-Seq Data Analysis

Sequenced reads were aligned to the mouse reference genome (mm9) and peak calling was performed with HOMER (Heinz et al., 2010). Sources of public ChIP-seq data analyzed are listed in Table S2B. See also Extended Experimental Procedures.

Liver-Specific Gene Expression

Flag-Rev-erbα and GFP cDNAs were subcloned into hepatocyte-specific AAV vector AAV8-Tbg (Bell et al., 2011) and tail veins were injected with 1×10^{12} genome copies per mouse. Livers were harvested 2 weeks after injection.

ACCESSION NUMBERS

The GEO accession number for the GRO-seq and ChIP-seq data reported in this paper is GSE59486. The GEO accession number for the microarray data reported in this paper is GSE59460.

SUPPLEMENTAL INFORMATION

Supplemental Information includes Extended Experimental Procedures, seven figures, and five tables and can be found with this article online at http://dx.doi.org/10.1016/j.cell.2014.10.022.

AUTHOR CONTRIBUTIONS

B.F., L.J.E., J.J., and M.A.L. conceived the project design and wrote the manuscript. B.F. performed analysis of GRO-seq data. B.F., L.J.E., and A.R. performed integrative genomic analyses. J.J. performed GRO-seq experiments. E.B. and L.J.E. performed E4BP4 ChIP-seq. D.F. performed RORα ChIP-seq. J.J., E.B., and Z.G.H. performed RT-qPCR and ChIP-qPCR experiments. S.M.A. and Z.S. performed AAV overexpression experiments.

ACKNOWLEDGMENTS

We thank the Functional Genomics Core (J. Schug and K. Kaestner) and Viral Vector Core (J. Johnston and A. Sandhu) of the Penn Diabetes Research Center (P30 DK19525) for next-generation sequencing and AAV production, respectively. We also thank the Penn Microarray Core for microarray analysis. We thank Dr. Ken Zaret for critical reading of the manuscript. This work was supported by NIH grants R01 DK45586 (M.A.L.), F32 DK095526 (L.J.E.), K99 DK099443 (Z.S.), and F32 DK095563 (Z.G.H.), and the JPB Foundation.

Received: April 21, 2014
Revised: August 28, 2014
Accepted: September 24, 2014
Published: November 20, 2014

REFERENCES

Adamovich, Y., Rousso-Noori, L., Zwighaft, Z., Neufeld-Cohen, A., Golik, M., Kraut-Cohen, J., Wang, M., Han, X., and Asher, G. (2014). Circadian clocks and feeding time regulate the oscillations and levels of hepatic triglycerides. Cell Metab. *19*, 319–330.

Anafi, R.C., Lee, Y., Sato, T.K., Venkataraman, A., Ramanathan, C., Kavakli, I.H., Hughes, M.E., Baggs, J.E., Growe, J., Liu, A.C., et al. (2014). Machine learning helps identify CHRONO as a circadian clock component. PLoS Biol. *12*, e1001840.

Asher, G., and Schibler, U. (2011). Crosstalk between components of circadian and metabolic cycles in mammals. Cell Metab. *13*, 125–137.

Bell, P., Gao, G., Haskins, M.E., Wang, L., Sleeper, M., Wang, H., Calcedo, R., Vandenberghe, L.H., Chen, S.J., Weisse, C., et al. (2011). Evaluation of adeno-associated viral vectors for liver-directed gene transfer in dogs. Hum. Gene Ther. *22*, 985–997.

Bugge, A., Feng, D., Everett, L.J., Briggs, E.R., Mullican, S.E., Wang, F., Jager, J., and Lazar, M.A. (2012). Rev-erbα and Rev-erbβ coordinately protect the circadian clock and normal metabolic function. Genes Dev. *26*, 657–667.

Cho, H., Zhao, X., Hatori, M., Yu, R.T., Barish, G.D., Lam, M.T., Chong, L.W., DiTacchio, L., Atkins, A.R., Glass, C.K., et al. (2012). Regulation of circadian behaviour and metabolism by REV-ERB-α and REV-ERB-β. Nature *485*, 123–127.

Ciarleglio, C.M., Resuehr, H.E., Axley, J.C., Deneris, E.S., and McMahon, D.G. (2014). Pet-1 deficiency alters the circadian clock and its temporal organization of behavior. PLoS ONE *9*, e97412.

Core, L.J., Waterfall, J.J., and Lis, J.T. (2008). Nascent RNA sequencing reveals widespread pausing and divergent initiation at human promoters. Science *322*, 1845–1848.

Cowell, I.G., Skinner, A., and Hurst, H.C. (1992). Transcriptional repression by a novel member of the bZIP family of transcription factors. Mol. Cell. Biol. *12*, 3070–3077.

Creyghton, M.P., Cheng, A.W., Welstead, G.G., Kooistra, T., Carey, B.W., Steine, E.J., Hanna, J., Lodato, M.A., Frampton, G.M., Sharp, P.A., et al. (2010). Histone H3K27ac separates active from poised enhancers and predicts developmental state. Proc. Natl. Acad. Sci. USA *107*, 21931–21936.

Dibner, C., Schibler, U., and Albrecht, U. (2010). The mammalian circadian timing system: organization and coordination of central and peripheral clocks. Annu. Rev. Physiol. *72*, 517–549.

Duez, H., van der Veen, J.N., Duhem, C., Pourcet, B., Touvier, T., Fontaine, C., Derudas, B., Baugé, E., Havinga, R., Bloks, V.W., et al. (2008). Regulation of bile acid synthesis by the nuclear receptor Rev-erbalpha. Gastroenterology *135*, 689–698.

Eckel-Mahan, K.L., Patel, V.R., de Mateo, S., Orozco-Solis, R., Ceglia, N.J., Sahar, S., Dilag-Penilla, S.A., Dyar, K.A., Baldi, P., and Sassone-Corsi, P. (2013). Reprogramming of the circadian clock by nutritional challenge. Cell *155*, 1464–1478.

Everett, L.J., Le Lay, J., Lukovac, S., Bernstein, D., Steger, D.J., Lazar, M.A., and Kaestner, K.H. (2013). Integrative genomic analysis of CREB defines a critical role for transcription factor networks in mediating the fed/fasted switch in liver. BMC Genomics *14*, 337.

Feng, D., Liu, T., Sun, Z., Bugge, A., Mullican, S.E., Alenghat, T., Liu, X.S., and Lazar, M.A. (2011). A circadian rhythm orchestrated by histone deacetylase 3 controls hepatic lipid metabolism. Science *331*, 1315–1319.

Gachon, F., Olela, F.F., Schaad, O., Descombes, P., and Schibler, U. (2006). The circadian PAR-domain basic leucine zipper transcription factors DBP, TEF, and HLF modulate basal and inducible xenobiotic detoxification. Cell Metab. *4*, 25–36.

Giguère, V., Tini, M., Flock, G., Ong, E., Evans, R.M., and Otulakowski, G. (1994). Isoform-specific amino-terminal domains dictate DNA-binding properties of ROR alpha, a novel family of orphan hormone nuclear receptors. Genes Dev. *8*, 538–553.

Gilardi, F., Migliavacca, E., Naldi, A., Baruchet, M., Canella, D., Le Martelot, G., Guex, N., and Desvergne, B.; CycliX Consortium (2014). Genome-wide analysis of SREBP1 activity around the clock reveals its combined dependency on nutrient and circadian signals. PLoS Genet. *10*, e1004155.

Hah, N., Murakami, S., Nagari, A., Danko, C.G., and Kraus, W.L. (2013). Enhancer transcripts mark active estrogen receptor binding sites. Genome Res. *23*, 1210–1223.

Harding, H.P., and Lazar, M.A. (1995). The monomer-binding orphan receptor Rev-Erb represses transcription as a dimer on a novel direct repeat. Mol. Cell. Biol. *15*, 4791–4802.

Hatanaka, F., Matsubara, C., Myung, J., Yoritaka, T., Kamimura, N., Tsutsumi, S., Kanai, A., Suzuki, Y., Sassone-Corsi, P., Aburatani, H., et al. (2010). Genome-wide profiling of the core clock protein BMAL1 targets reveals a strict relationship with metabolism. Mol. Cell. Biol. *30*, 5636–5648.

Heinz, S., Benner, C., Spann, N., Bertolino, E., Lin, Y.C., Laslo, P., Cheng, J.X., Murre, C., Singh, H., and Glass, C.K. (2010). Simple combinations of lineage-determining transcription factors prime cis-regulatory elements required for macrophage and B cell identities. Mol. Cell *38*, 576–589.

Hollenhorst, P.C., McIntosh, L.P., and Graves, B.J. (2011). Genomic and biochemical insights into the specificity of ETS transcription factors. Annu. Rev. Biochem. *80*, 437–471.

Hughes, M.E., DiTacchio, L., Hayes, K.R., Vollmers, C., Pulivarthy, S., Baggs, J.E., Panda, S., and Hogenesch, J.B. (2009). Harmonics of circadian gene transcription in mammals. PLoS Genet. *5*, e1000442.

Hughes, M.E., Hogenesch, J.B., and Kornacker, K. (2010). JTK_CYCLE: an efficient nonparametric algorithm for detecting rhythmic components in genome-scale data sets. J. Biol. Rhythms *25*, 372–380.

Kim, T.K., Hemberg, M., Gray, J.M., Costa, A.M., Bear, D.M., Wu, J., Harmin, D.A., Laptewicz, M., Barbara-Haley, K., Kuersten, S., et al. (2010). Widespread transcription at neuronal activity-regulated enhancers. Nature *465*, 182–187.

Koike, N., Yoo, S.H., Huang, H.C., Kumar, V., Lee, C., Kim, T.K., and Takahashi, J.S. (2012). Transcriptional architecture and chromatin landscape of the core circadian clock in mammals. Science *338*, 349–354.

Kornmann, B., Schaad, O., Bujard, H., Takahashi, J.S., and Schibler, U. (2007). System-driven and oscillator-dependent circadian transcription in mice with a conditionally active liver clock. PLoS Biol. *5*, e34.

Lam, M.T., Cho, H., Lesch, H.P., Gosselin, D., Heinz, S., Tanaka-Oishi, Y., Benner, C., Kaikkonen, M.U., Kim, A.S., Kosaka, M., et al. (2013). Rev-Erbs repress macrophage gene expression by inhibiting enhancer-directed transcription. Nature *498*, 511–515.

Li, S., and Hunger, S.P. (2001). The DBP transcriptional activation domain is highly homologous to that of HLF and TEF and is not responsible for the tissue type-specific transcriptional activity of DBP. Gene *263*, 239–245.

Li, W., Notani, D., Ma, Q., Tanasa, B., Nunez, E., Chen, A.Y., Merkurjev, D., Zhang, J., Ohgi, K., Song, X., et al. (2013). Functional roles of enhancer RNAs for oestrogen-dependent transcriptional activation. Nature *498*, 516–520.

Menet, J.S., Rodriguez, J., Abruzzi, K.C., and Rosbash, M. (2012). Nascent-Seq reveals novel features of mouse circadian transcriptional regulation. eLife *1*, e00011.

Miller, B.H., McDearmon, E.L., Panda, S., Hayes, K.R., Zhang, J., Andrews, J.L., Antoch, M.P., Walker, J.R., Esser, K.A., Hogenesch, J.B., and Takahashi, J.S. (2007). Circadian and CLOCK-controlled regulation of the mouse transcriptome and cell proliferation. Proc. Natl. Acad. Sci. USA *104*, 3342–3347.

Mitsui, S., Yamaguchi, S., Matsuo, T., Ishida, Y., and Okamura, H. (2001). Antagonistic role of E4BP4 and PAR proteins in the circadian oscillatory mechanism. Genes Dev. *15*, 995–1006.

Panda, S., Antoch, M.P., Miller, B.H., Su, A.I., Schook, A.B., Straume, M., Schultz, P.G., Kay, S.A., Takahashi, J.S., and Hogenesch, J.B. (2002). Coordinated transcription of key pathways in the mouse by the circadian clock. Cell *109*, 307–320.

Peek, C.B., Ramsey, K.M., Marcheva, B., and Bass, J. (2012). Nutrient sensing and the circadian clock. Trends Endocrinol. Metab. *23*, 312–318.

Reppert, S.M., and Weaver, D.R. (2001). Molecular analysis of mammalian circadian rhythms. Annu. Rev. Physiol. *63*, 647–676.

Rey, G., Cesbron, F., Rougemont, J., Reinke, H., Brunner, M., and Naef, F. (2011). Genome-wide and phase-specific DNA-binding rhythms of BMAL1 control circadian output functions in mouse liver. PLoS Biol. *9*, e1000595.

Ripperger, J.A., and Schibler, U. (2001). Circadian regulation of gene expression in animals. Curr. Opin. Cell Biol. *13*, 357–362.

Ripperger, J.A., and Schibler, U. (2006). Rhythmic CLOCK-BMAL1 binding to multiple E-box motifs drives circadian Dbp transcription and chromatin transitions. Nat. Genet. *38*, 369–374.

Seo, Y.K., Chong, H.K., Infante, A.M., Im, S.S., Xie, X., and Osborne, T.F. (2009). Genome-wide analysis of SREBP-1 binding in mouse liver chromatin reveals a preference for promoter proximal binding to a new motif. Proc. Natl. Acad. Sci. USA *106*, 13765–13769.

Step, S.E., Lim, H.W., Marinis, J.M., Prokesch, A., Steger, D.J., You, S.H., Won, K.J., and Lazar, M.A. (2014). Anti-diabetic rosiglitazone remodels the adipocyte transcriptome by redistributing transcription to PPARγ-driven enhancers. Genes Dev. *28*, 1018–1028.

Takahashi, J.S., Hong, H.K., Ko, C.H., and McDearmon, E.L. (2008). The genetics of mammalian circadian order and disorder: implications for physiology and disease. Nat. Rev. Genet. *9*, 764–775.

Tong, X., Muchnik, M., Chen, Z., Patel, M., Wu, N., Joshi, S., Rui, L., Lazar, M.A., and Yin, L. (2010). Transcriptional repressor E4-binding protein 4 (E4BP4) regulates metabolic hormone fibroblast growth factor 21 (FGF21) during circadian cycles and feeding. J. Biol. Chem. *285*, 36401–36409.

Ueda, H.R., Hayashi, S., Chen, W., Sano, M., Machida, M., Shigeyoshi, Y., Iino, M., and Hashimoto, S. (2005). System-level identification of transcriptional circuits underlying mammalian circadian clocks. Nat. Genet. *37*, 187–192.

Ukai-Tadenuma, M., Kasukawa, T., and Ueda, H.R. (2008). Proof-by-synthesis of the transcriptional logic of mammalian circadian clocks. Nat. Cell Biol. *10*, 1154–1163.

Vollmers, C., Gill, S., DiTacchio, L., Pulivarthy, S.R., Le, H.D., and Panda, S. (2009). Time of feeding and the intrinsic circadian clock drive rhythms in hepatic gene expression. Proc. Natl. Acad. Sci. USA *106*, 21453–21458.

Wang, D., Garcia-Bassets, I., Benner, C., Li, W., Su, X., Zhou, Y., Qiu, J., Liu, W., Kaikkonen, M.U., Ohgi, K.A., et al. (2011). Reprogramming transcription by distinct classes of enhancers functionally defined by eRNA. Nature *474*, 390–394.

Yoshitane, H., Ozaki, H., Terajima, H., Du, N.H., Suzuki, Y., Fujimori, T., Kosaka, N., Shimba, S., Sugano, S., Takagi, T., et al. (2014). CLOCK-controlled polyphonic regulation of circadian rhythms through canonical and noncanonical E-boxes. Mol. Cell. Biol. *34*, 1776–1787.

Zhao, Q., Khorasanizadeh, S., Miyoshi, Y., Lazar, M.A., and Rastinejad, F. (1998). Structural elements of an orphan nuclear receptor-DNA complex. Mol. Cell *1*, 849–861.

Zhao, X., Cho, H., Yu, R.T., Atkins, A.R., Downes, M., and Evans, R.M. (2014). Nuclear receptors rock around the clock. EMBO Rep. *15*, 518–528.